# Nonlinear Model Predictive Control for Autonomous Sailboat with Optimization of Sail Angle

Junzhuo Wu, Ya-Jun Pan, Chao Shen, Sean Smith, Emmanuel Witrant

# Nonlinear Model Predictive Control for Autonomous Sailboat with Optimization of Sail Angle

Junzhuo Wu[1], Ya-Jun Pan[1], *Senior Member, IEEE,* Chao Shen[2], *Member, IEEE,*
Sean Smith[3], *Student Member, IEEE,* and Emmanuel Witrant[3]

***Abstract*—This paper studies trajectory tracking control problems of sailing vessels using a nonlinear model predictive control (NMPC) approach with a novel sail angle optimization approach. The proposed sail angle optimization method accounts for physical constraints during practical implementation such as operational sail angle bound and rate of change in sail angles. This technique also emphasizes the potential to use the sail to plan a safe trajectory, while a simple proportional-derivative (PD) controller is used for rudder angle regulation. The NMPC is implemented for trajectory tracking control in the simulation. Results show that the proposed controller can achieve excellent tracking performance in the presence of environmental disturbances in terms of ocean waves.**

***Keywords*—Autonomous Sailboat; Nonlinear Model Predictive Control; Sail Angle Optimization; Trajectory Tracking; Robust Control**

## I. Introduction

Autonomous sailboats represent a rising frontier in future marine technology, offering potential applications ranging from oceanographic research to sea transportation. Unlike traditional sailboats, autonomous sailboats operate without human intervention, navigating and performing tasks autonomously using preset algorithms and control logic.

The control of autonomous sailboats has been receiving increasing attention from academics. With only two controllable components, the sail and rudder, the underactuated nature of the boat makes position and speed control a challenging task. Sail angle determination in conventional autonomous sailboat motion control has not been as extensively studied as rudder control in recent years. This is because the rudder predominantly contributes to yaw angle adjustments, while the sail mainly provides thrusts. In many cases, the manipulation of sailing speed in sailboat control is overlooked since higher priorities are given to trajectory tracking.

As one of the two sole thrust providers, the optimal control of the sail deserves further investigation. An appropriate sail angle could facilitate tracking manoeuvre while regulating excessive roll angles and significantly improve sailboat speed when paired with sufficient rudder control. Conventionally, sail angles are simply selected from three possible numerical values based on the relationship between the heading and apparent wind angles [1]. This leaves considerable potential to increase the adaptability of sail angles to accommodate instantaneous trajectory change, along with speed considerations. A sail angle optimization logic that finds the sailboat's maximum forward thrust which generates the highest travelling speed is introduced in [2]. In [3], a systematic approach using the Extremum Seeking controller maximizes the longitudinal velocity of a surface sailing vehicle by changing the angle of the sail. In [4], a simple model-free sail angle control maximizer was included. However, the above-listed approaches often overlook physical constraints of the sail such as sail angle ranges and sail angle switching rate, which hinders the control practicality and feasible implementation onto actual sailboat models.

The control of sailboats to perform tasks such as trajectory tracking presents a unique set of challenges due to their highly coupled and nonlinear dynamics. Such characteristics demand a model-based controller to be adopted. Model predictive control (MPC), also known as receding horizon control, is an advanced control strategy that optimizes the control inputs by solving a finite horizon optimization problem at each time step and recursively finds the optimal solution on a rolling basis. MPC possesses a strong ability in constraint handling, which makes this approach particularly suitable for controlling autonomous sailboats in complex ocean environments. For MPC of sailboats only a few pioneering works are reported in the literature [5], [6]. Notably, [5] has proposed a linearized MPC for sailboat position control. However, large modelling errors and process noises could arise from the linearization of highly coupled nonlinear sailboat model dynamics. In such regard, the nonlinear extension NMPC appears more competent as a robust controller subjected to unknown disturbances such as waves and time-varying moving masses. The use of NMPC has been broadly reported in other marine applications [7]. An approach to integrate path planning and tracking control of an autonomous underwater vehicle (AUV) using NMPC is reported in [8] and extended Lyapunov-based NMPC [9]. Reinforcement Learning-based NMPC has been applied to autonomous surface vehicle (ASV) [10].

In this work, we first propose a model-based approach for sailboat longitudinal speed maximization for autonomous sailboats. The approach builds on the work in [2] and extends with sail angle range considerations. Then we take the generated optimized sail angle as input for the NMPC trajectory tracking problem. The proposed control system consists of

This work is supported by the Natural Sciences and Engineering Research Council (NSERC).

[1]J. Wu and Y.J. Pan are with the Advanced Control and Mechatronics Lab, Department of Mechanical Engineering, Dalhousie University, Halifax, Canada, B3H 4R2. (jn574392@dal.ca), (yajun.pan@dal.ca). [2]C. Shen is with the Department of Systems and Computer Engineering, Carleton University, Ottawa, K1S-5B6, Canada. (shenchao@sce.carleton.ca). [3]S. Smith and E. Witrant are with the GIPSA-lab, CNRS, University of Grenoble Alpes, F-38000 Grenoble, France. (s.smith@dal.ca), (emmanuel.witrant@univ-grenoble-alpes.fr).

two main loops, as shown in Fig. 1. The first loop generates optimized sail angles and calculates the rudder angle (from a complementary controller) and state variables based on the sailboat kinetics and kinematics model. The state variables are then fed back to the sail angle optimization problem as parameters. A full set of trajectories is passed to the second loop as reference states and inputs for the NMPC tracking control.

## II. System Description

### A. Notations

The following notations are used in this paper:

- $x, y, \phi, \psi$: translations and rotations (roll and yaw) in n-frame;
- $u, v, p, r$: translational and angular velocities in b-frame;
- $\alpha_{tw}, \alpha_{aw}, \alpha_s$: direction of true/apparent wind, sail angle of attack;
- $v_{tw}, v_{aw}$: speed of true/apparent wind;
- $\delta_s, \delta_r$: sail angle, rudder angle;
- $C_s^T(\cdot), C_s^N(\cdot)$: Tangential and normal force generated from sail;
- $C_s^L(\cdot), C_s^D(\cdot)$: lift and drag coefficient of the sail;
- $\rho_{air}, \rho$: density of air and surrounding water;
- $A_s$: surface area of the sail.

### B. Sailboat Model

The sailboat apparatus can be represented using a 4-degree-of-freedom (4-DOF) model [11] as shown in Fig. 2. It is assumed that the pitch and vertical motion are negligible compared to other motions, such that the 4-DOF dynamics represent $x, y$ translations and $\phi, \psi$ rotations. The north-east-down coordinate system is designated as the inertial frame (n-frame) and the body-fixed frame (b-frame) is to be the rotated reference frame attached to the ship body. The angular velocities, $[p, r]^T$, are relative to the n-frame. The origin of the n-frame and b-frame coincide.

Vector $\eta = [x, y, \phi, \psi]^T$ is used to describe the position and angles of the sailboat in n-frame and $v = [u, v, p, r]^T$ denotes their corresponding generalized velocity in b-frame.

A classical rigid-body dynamics equation for sailboats introduced in [11] is presented as in Eq. (1):

$$M_{RB}\dot{v} + C_{RB}(v)v = \tau_{RB}, \tag{1}$$

where $M_{RB} \in \mathbb{R}^{4\times4}$ represents the rigid-body inertial matrix, and $C_{RB} \in \mathbb{R}^{4\times4}$ represents the rigid-body Coriolis and centripetal matrix.

As the sailboat is actively travelling in water, the additional force and moment generated by the inertia of the surrounding water flow, namely the added mass effects, also need to be taken into consideration. Similarly, we define the resulting added mass inertial and Coriolis matrices to be $M_A$ and $C_A$, respectively. The overall inertial matrix $M$ is defined as $M = M_{RB} + M_A$. Analogously, $C = C_{RB} + C_A$. Finally, we can establish the comprehensive representation of the sailboat dynamics as:

$$M\dot{v} + C(v)v + D(v, \eta) + g(\eta) = \tau, \tag{2}$$

where $D(v, \eta)$ is the damping matrix, and $g(\eta)$ is the restoring torque matrix. $\tau$ contains forces and moments generated from the sail and rudder used to control the boat and inherently depends on $\eta$ and $v$. Additionally, the wind velocity and direction along with the two control inputs, sail angle $\delta_s$ and rudder angle $\delta_r$, also affect $\tau$.

The n-frame position and angle vector $\eta$ are correlated to the b-frame velocity vector $v$ by a transformation vector $J(\eta)$, $\dot{\eta} = J(\eta)v$ [11].

The state-space representation of the sailboat model is then obtained by inverting inertial matrix $M$, as shown in Eq.(3)

$$\begin{aligned} \dot{\eta} =& J(\eta)v, \\ \dot{v} =& -M^{-1}C(v)v - M^{-1}D(v, \eta) \\ & - M^{-1}g(\eta) + M^{-1}\tau(\eta, v, \delta_r, \delta_s, v_{tw}, \alpha_{tw}). \end{aligned} \tag{3}$$

## III. Control Design

### A. Sail Angle Optimization

In [2], Saoud et al. introduced an optimization structure that optimizes the travelling speed of sailboats by maximizing the longitudinal thrust force generated by the sail. This method sets constraints on roll moments, which improves the cruise stability of the vehicle. The optimization problem can be interpreted as below:

$$\max \quad F_{s,forward} \quad s.t.\ M_{xs} = g(\eta), \tag{4}$$

where $F_{s,forward}$ denotes the longitudinal forward thrust provided by the sail, and $M_{xs}$ represents the sail-generated roll moment. Since sail angle $\delta_s$ is the only input to sail-provided forces and moments, it is crucial to express Eq. (4) as a function of $\delta_s$.

The sail force can be represented as [2]:

$$\begin{aligned} F_s =& -\frac{1}{2}\rho_{air}A_sC_s^N(sin(\alpha_s))\|u^2 + v^2\|\vec{j} \\ & -\frac{1}{2}\rho_{air}A_sC_s^T(sin(\alpha_s))\|u^2 + v^2\|\vec{i}, \end{aligned} \tag{5}$$

where $\vec{i}, \vec{j}$ denote tangential and normal direction to the sail plane. $C_s^T(\alpha_s)$ and $C_s^N(\alpha_s)$ are polynomials that use $\sin(\alpha_s)$ to represent tangential and normal forces. It is concluded from [12] that the magnitude of $C_s^T \ll C_s^N$ on sails, when satisfying conditions of sails having high aspect ratio and low camber.

Thus the sail force (5) can be simplified as:

$$F_s \simeq -\frac{1}{2}\rho_{air}A_sC_s^N(sin(\alpha_s))\|u^2 + v^2\|. \tag{6}$$

The thrust force that propels the sailboat to travel forward in the longitudinal direction and the roll moment generated by the sail are then found to be:

$$\begin{cases} F_{s,forward} = -\frac{1}{2}\rho_{air}A_sC_s^N(sin(\alpha_s))\|u^2 + v^2\|sin(\delta_s) \\ M_{xs} = -\frac{1}{2}h_s\rho_{air}A_sC_s^N(sin(\alpha_s))\|u^2 + v^2\|cos(\delta_s), \end{cases} \tag{7}$$

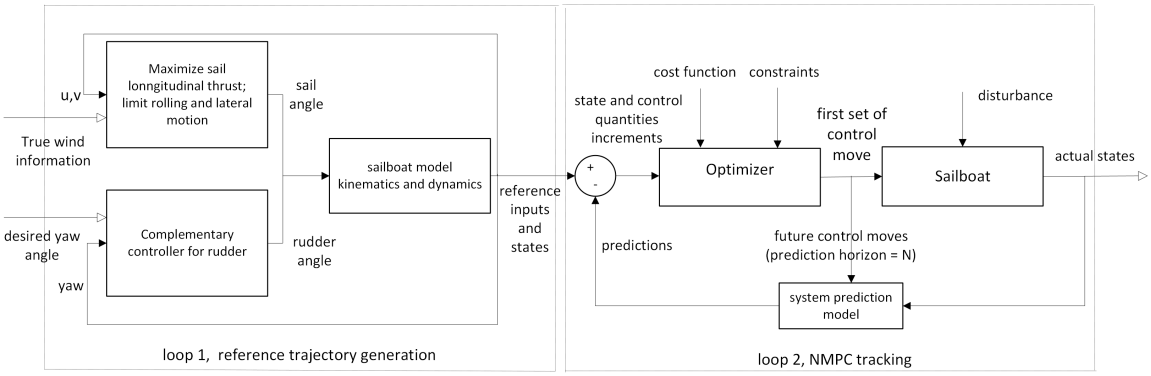


Fig. 1: Sailboat control flow block diagram

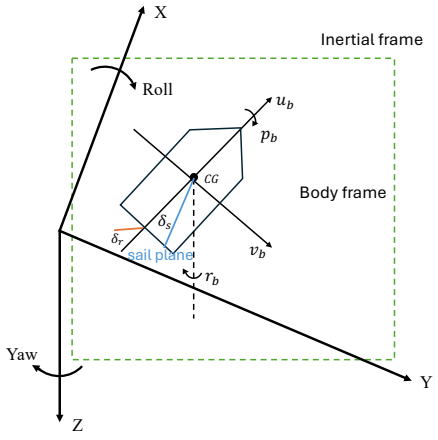


Fig. 2: Sailboat 4-DOF model

where $h_s$ is the vertical distance between the centre of gravity of the entire boat and one of the sails alone.

The angle of attack $\alpha_s$ depends on the sail angle $\delta_s$ as $\alpha_s = \alpha_{aw} - \delta_s$.

The optimization problem (4) for any given apparent wind direction $\alpha_{aw}$ can then be rewritten as:

$$\begin{aligned} \min_{\delta_s} \quad & f(sin(\alpha_{aw} - \delta_s))sin(\delta_s) \\ s.t. \quad & f(sin(\alpha_{aw} - \delta_s))cos(\delta_s) = \frac{g(\eta)}{\lambda}, \\ \text{where } & f(sin(\alpha_{aw} - \delta_s)) = C_s^N(sin(\alpha_{aw} - \delta_s)) \\ \text{and } & \lambda = -\frac{1}{2}h_s\rho_{air}A_s\|u^2 + v^2\|, \end{aligned} \tag{8}$$

Eq.(8) is solved spontaneously and iteratively while the boat is travelling forward with continuously updated $\alpha_{aw}$ calculated from boat kinematics and dynamics.

We now introduce the concept of limited sail angle bounds to this optimization problem. In practice, the maximum sail angle is determined by ribbing constraints: the maximum available length of the sheet which connects the sail to its actuator and standing rigging. Empirically, sailors would change the sheet length, which "tunes" the maximum sail angle to obtain faster/slower travelling speed.

Instead of directly discarding solutions numerically larger than the maximum allowed sail angle, the proposed approach is to post-process solutions obtained from solving (8) and then compare sail angle bound constraint with the computed angles. This process is illustrated as follows:

**Algorithm 1**

$k = 1$
**for** $k \leq T$ **do**
  **if** $|\delta_s| \geq \pi$ **then** ▷ Convert $\delta_s \in [-\pi, \pi]$
    $\delta_s = mod(\delta_s + \pi, 2\pi) \mp \pi$
  **end if**
  **if** $\bar{\delta_s} \leq \frac{\pi}{2}$ **then** ▷ If allowed max. $\delta_s$ is less than $\frac{\pi}{2}$
    **if** $|(\delta_s)| \geq \frac{\pi}{2}$ **then** ▷ Convert $\delta_s \in [-\frac{\pi}{2}, \frac{\pi}{2}]$
      $\delta_s = \delta_s \mp \pi$
    **end if**
  **end if**
  $\delta_s = sat_{-\bar{\delta_s}}^{\bar{\delta_s}}(\delta_s)$
  $k = k + 1$
**end for**

### B. NMPC Algorithm

Given the optimal trajectory planned using the method described in Section A, we then implement NMPC to perform trajectory-tracking tasks.

The dynamics and kinematics equation (3) can be expressed as the nonlinear equation:

$$\dot{x} = \begin{bmatrix} J(\eta)v \\ -M^{-1}(Cv + D + g - \tau) \end{bmatrix} = f(x, u), \tag{9}$$

where $x = [x, y, \phi, \psi, u, v, p, r]^T$ represents the n-frame state quantities and $u = [\delta_r, \delta_s]^T$ control quantities in b-frame.

Since MPC requires a discrete-time model, (9) is discretized using, for example, the Forward Euler method.

$$x(k+1) = f_d(x(k), u(k)). \tag{10}$$

Consider a desired trajectory $x_d(k) = [x_d, y_d, \phi_d, \psi_d, u_d, v_d, p_d, r_d]^T$ that defines the reference position and velocity of the sailboat. The corresponding

reference rudder and sail angles are defined as $u_d = [\delta_{rd}, \delta_{sd}]^T$.

A quadratic cost function formulation for sailboat trajectory tracking control can be then established as follows:

$$\begin{aligned} \min_{u} \quad & J = \sum_{0}^{T} \|x_e(k)\|_Q^2 + \|u_e(k)\|_R^2 + \|\delta_r\|_F^2 + \|x(T)\|_D^2 \\ s.t. \quad & x(k+1) = f(x(k), u(k)) \\ & x(0) = x(t_0) \\ & |x_e(k)| \leq x_{e,max} \\ & |u_e(k)| \leq u_{e,max}, \end{aligned} \tag{11}$$

where $x_e = x - x_d$ is the error state and $u_e = u - u_d$ is the control error, T is the prediction horizon; $\|x(T)\|_D^2$ is the terminal state penalty and the weighting matrices Q, R, F, and D are positive definite. The stage cost terms $\|x_e(k)\|_Q^2$ and $\|u_e(k)\|_R^2$ drive the actual states and inputs to converge to their corresponding references; the third term $\|\delta_r\|_F^2$ helps the rudder angle to reach zero faster.

## IV. Performance Evaluation

In this section, simulation results for sail angle optimization and NMPC trajectory tracking are presented. The algorithms are written in MATLAB using the CasADi framework. Simulations are carried out to simulate a 12-m class sailboat [1].

### A. Sail Angle Optimization

In this subsection, we compare the simulation results of the proposed optimized sail angle planning technique with the generic sail angle selector method, as documented in earlier works [1] [13]. Circumstances of side-wind sailing and jibing subjected to different wind conditions are applied and studied. To demonstrate the effectiveness of the proposed sail angle optimization scheme, identical PD controllers are deployed on the rudder for both sail angle planners. Due to the simplicity of the generic sail angle selector method, the robustness of the sails is usually guaranteed by robust rudder controllers, which play a major role in stabilizing the whole vehicle. In the following section, we evaluate the capability of our proposed sail angle optimizer to be the main contributor to safe sailing.

*1) Side-wind Sailing:* Side-wind sailing is the most common way of sailing, allowing boats to steadily travel forward when the wind is near-perpendicular to the sailboat body. In this case, the true wind is simulated to blow from north to south with velocities of 6 m/s and 9 m/s, ie. $\alpha_{tw} = \pi$ and $v_{tw} \in \{6, 9\}$m/s. The desired heading is $\psi_d = \frac{\pi}{2}$. Both simulations assume an initial velocity of $u(0)$ = 2 m/s and an initial boat direction facing south $\psi(0) = \pi$. The PD controller gain terms are $[k_1, k_2]^T = [0.9, 1]^T$. The maximum allowed sail angle is $\bar{\delta_s} = \frac{\pi}{4}$.

Fig. 3(a) shows that the proposed sail angle optimization technique can provide clear $\delta_s$ switching when a drastic $\delta_s$ change is needed with the absence of a robust rudder controller. In opposition to the proposed technique, the generic sail angle selector method hesitates to do so, by rapidly switching

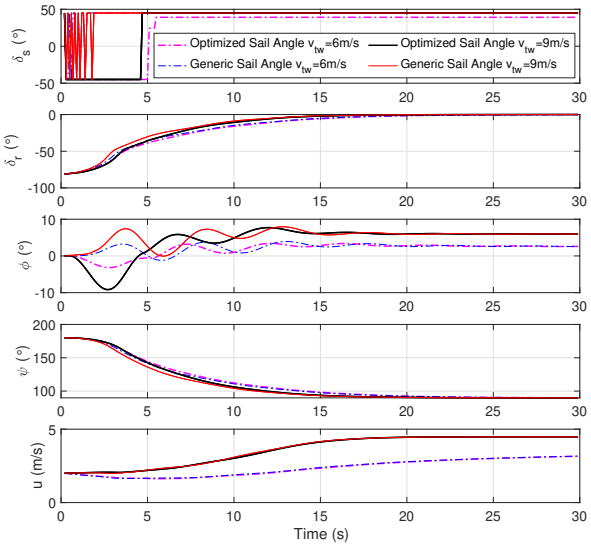


(a) Time evolution of $\delta_r, \delta_s, \phi, \psi, u$ comparison with different wind speed (side-wind maneuver)

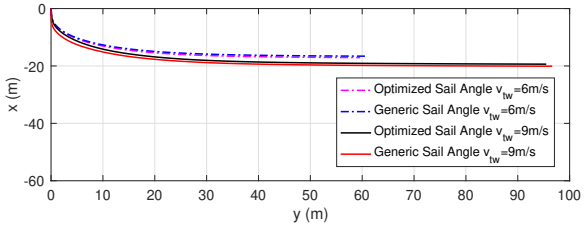


(b) Trajectory comparison with different wind speed (side-wind maneuver)

Fig. 3: Sail angle generation of the side-wind maneuver

from upper $\delta_s$ bound to lower $\delta_s$ bound before settling at a steady value. Eliminating such rapid $\delta_s$ change is desired in practical applications due to the physical limitation of the sail actuator. Using the sail angle optimization technique, the missing constant $\delta_s$ switching element, which balances the boat, is compensated by slightly larger $\phi$ in the first 5 seconds. Yet the roll moment constraint present in the optimization process quickly helps $\phi$ to settle. Fig. 3(a) shows the consequential trajectories subject to both sail angle selection techniques. Within a simulation duration of 30 seconds, the proposed method travels 0.91 m (1.4%) less distance in the desired direction. However the longitudinal speed $u$ is slowly catching up by 0.013 m/s at the end of the simulation. Such difference is less pronounced with higher wind speed when $\alpha_{tw}$ = 9 m/s.

When $v_{tw}$ = 9 m/s, the significant fluctuation of $\delta_s$ obtained from the generic sail angle method lasts noticeably longer, which is even less ideal for practical implementation. As a comparison, a crisp change of $\delta_s$ is generated from our proposed technique. The proposed sail angle optimization method also allows for more subtle rolling motion and converges to a steady state faster. The discrepancy of displacement is 1.15 m (1.07%) by the time the simulation ends. Longitudinal speed $u$ from the generic sail angle method was slightly higher in

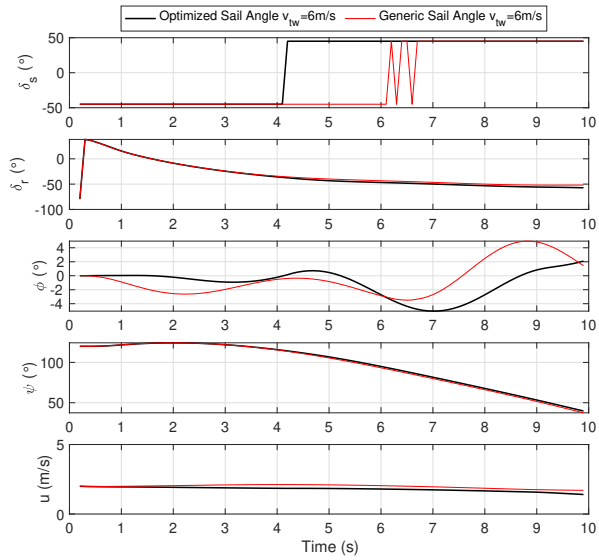


(a) Time evolution of $\delta_r, \delta_s, \phi, \psi, u$ when $v_{tw}$= 6m/s (jibing maneuver)

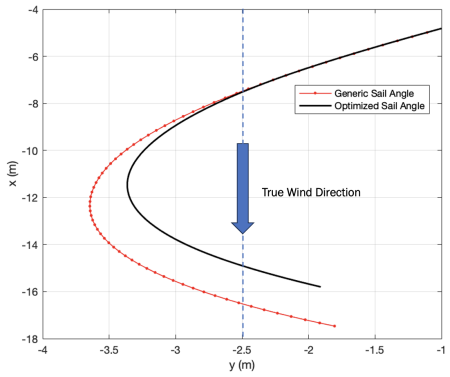


(b) Trajectory comparison when when $v_{tw}$= 6m/s (jibing maneuver)

Fig. 4: Sail angle generation of the jibing maneuver

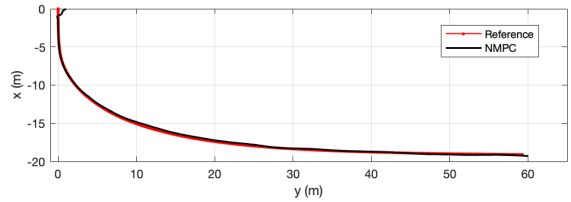


(a) Side-wind Trajectory Tracking

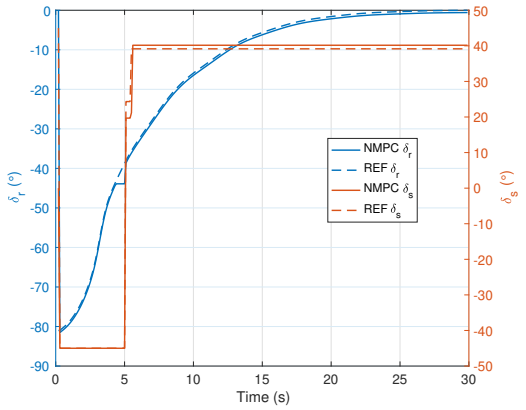


(b) Time Evolution of Side-wind Sailing Inputs

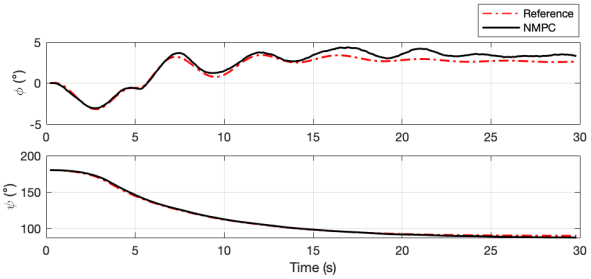


(c) Side-wind Sailing Angle Tracking

Fig. 5: Trajectory tracking of the side-wind maneuver

the first half of the journey (shown in the enlarged region), yet soon caught up by $u$ from the proposed method.

*2) Jibing:* The ability of the proposed method to generate a safe jibing trajectory is now evaluated. The true wind is simulated to blow from north to south $\alpha_{tw} = \frac{\pi}{2}$ with $v_{tw}$ = 6 m/s. The initial velocity is $u(0)$ = 2 m/s. The gain terms for the rudder PD controller are $[k_1, k_2]^T = [2, 1]^T$. The maximum allowed sail angle is $\bar{\delta_s} = \frac{\pi}{4}$.

As before, in Fig. 4(a), $\delta_s$ generated by the proposed method is much more favourable in terms of actuation constraints. Less fluctuation on the roll angle $\phi$ is also observed. In Fig. 4(b), it is seen that the turning radius in the trajectory is drastically less when using the proposed sail angle optimization tool. This suggests an easier jibing maneuver. We can thus conclude that our method improves sailing comfort, with samll difference in the total displacement.

### B. NMPC Algorithm Implementation

In this subsection, simulation results using the proposed NMPC method for sailboat system tracking with external disturbances are given. The parameters of the NMPC controller are chosen to achieve optimal trajectory tracking results. The discrete time step is $\delta$ = 0.1s, the prediction horizon is T = $10\delta$. Q = diag$(q_{11}, q_{22}, q_{33}, q_{44}, q_{55}, q_{66}, q_{77}, q_{88})$ = $2 \times 10^3$ $\mathbf{I}_8$, R = diag$(r_{11}, r_{22})$ = 0.5 $\mathbf{I}_2$, F = 0.1, D = diag$(qd_{11}, qd_{22}, qd_{33}, qd_{44}, qd_{55}, qd_{66}, qd_{77}, qd_{88})$= $5 \times 10^3$ $\mathbf{I}_8$.

The reference trajectories of the afore-determined side-wind sailing and jibing are applied and studied. The external disturbances are modelled to simulate perturbations caused by waves. Waves are assumed to be fully developed and modelled with a significant height of 1 m, which is the most commonly seen type of wave in the Atlantic Ocean environment [11].

*1) Side-wind Sailing:* The trajectory tracking ability along with the robustness of NMPC is tested in this section. $v_{tw} =$ 6 m/s, $\alpha_{tw} = \pi$, $\psi_d = \frac{\pi}{2}$. The initial states are $\mathbf{x}_0 = [0, 0.5, 0, \pi, 2, 0, 0, 0]^T$.

Fig. 5(a) shows that the initial error is quickly corrected and the reference trajectory is overall well-tracked. It is observed

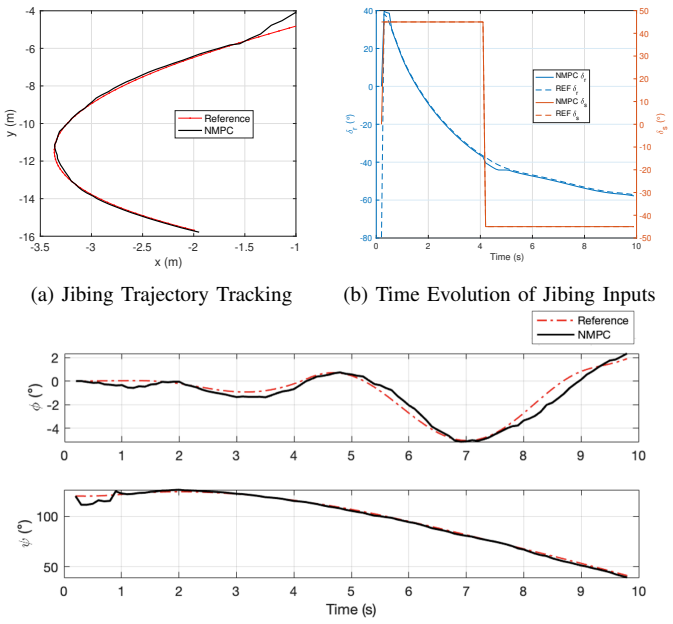


(a) Jibing Trajectory Tracking

(b) Time Evolution of Jibing Inputs

(c) Jibing Angle Tracking

Fig. 6: Trajectory tracking of the jibing maneuver

in Fig. 5(c) that introduced wave disturbance has caused noticeable disturbance to vehicle roll motion $\phi$, yet successfully recovered by NMPC and settles at approximately $3.42°$ and error between actual and reference roll angle $\phi_{error} = 0.84°$. Some minor discrepancies (approx. $\pm 10\%$) are also reported in yaw motion $\psi$, which are compensated by NMPC as well. The end yaw angle is $\psi(\infty) = 87.96°$ and $\psi_{error} = 2.09°$. Fig.5(b) illustrated the time evolution of two input angles, $\delta_r$ and $\delta_s$. The two reference inputs followed the patterns from their corresponding references but with slight adjustments to help with vehicle stabilization, $\delta_{r,offset}(\infty) = -0.69°$ and $\delta_{s,offset}(\infty) = 1.02°$. Notice at approximately 5 seconds, both $\delta_r$ and $\delta_s$ show larger variations compared to their references. This is due to the occurrence of a sharp turn accompanied by random disturbances.

*2) Jibing:* The robustness and ability to track a jibing trajectory are studied in this section. $v_{tw} = 6$ m/s, $\alpha_{tw} = \frac{\pi}{2}$. The initial states are $\mathbf{x}_0 = [-1, -4, 0, \frac{2\pi}{3}, 2, 0, 0, 0]^T$.

The jibing case is inherently more challenging due to the lowered travelling speed to perform the jibing maneuver with the presence of moderate wave disturbances. The position tracking result is shown in Fig. 6(a). The initial state error quickly converges and the rest of the trajectory is overall followed. A larger error can be seen in the region where $\dot{\psi}$ is the largest. Fig. 6(c) shows adequate constraints provided by NMPC to overcome angle disturbances, with average $\phi_{error}$ = 0.165 °, root mean square error $\phi_{RMSE}$ = 0.4125 °; average $\psi_{error}$ = 0.936 °, root mean square error $\psi_{RMSE}$ = 1.2376 °. The perturbations are mainly compensated by a minor offset in $\delta_r$, as shown in Fig. 6(b).

## V. Conclusion and Future Work

In this paper, we have presented an innovative approach combining sail angle optimization with bounded sail angles and NMPC for trajectory tracking of a sailing vessel. By integrating the optimization of sail angle with the NMPC framework, both control performance and robustness are enhanced. Simulation results of generating and tracking various trajectories highlight the advantages of the proposed method in sail angle optimization and trajectory tracking control.

In the near future, experiments on a real sailboat will be conducted to verify the proposed method. Furthermore, we are interested in enhancing the closed-loop properties of the nonlinear MPC tracking control system by integrating features of other control methods such as adaptive control [14], and neural-network-based control [15].

## References


[1] L. Xiao and J. Jouffroy, "Modeling and nonlinear heading control of sailing yachts," *IEEE Journal of Oceanic Engineering*, vol. 39, no. 2, pp. 256–268, 2014.

[2] H. Saoud, M.-D. Hua, F. Plumet, and F. Ben Amar, "Optimal sail angle computation for an autonomous sailboat robot," in *2015 54th IEEE Conference on Decision and Control (CDC)*, 2015, pp. 807–813.

[3] L. Xiao, J. C. Alves, N. A. Cruz, and J. Jouffroy, "Online speed optimization for sailing yachts using extremum seeking," in *2012 Oceans*, 2012, pp. 1–6.

[4] C. Viel, U. Vautier, J. Wan, and L. Jaulin, "Position keeping control of an autonomous sailboat," *IFAC-PapersOnLine*, vol. 51, pp. 14–19, 01 2018.

[5] S. Liu, Z. Yu, T. Wang, Y. Chen, Y. Zhang, and Y. Cai, "Mpc-based collaborative control of sail and rudder for unmanned sailboat," *Journal of Marine Science and Engineering*, vol. 11, no. 2, 2023.

[6] Y. Tipsuwan, P. Sanposh, and N. Techajaroonjit, "Overview and control strategies of autonomous sailboats—a survey," *Ocean Engineering*, vol. 281, p. 114879, 2023.

[7] A.-F. Fontaine, D. Zhu, N. Chen, and Y.-J. Pan, "Nonlinear model predictive control for autonomous underwater vehicle trajectory tracking," in *2023 IEEE 2nd Industrial Electronics Society Annual On-Line Conference (ONCON)*, 2023, pp. 1–6.

[8] C. Shen, Y. Shi, and B. Buckham, "Integrated path planning and tracking control of an auv: A unified receding horizon optimization approach," *IEEE/ASME Transactions on Mechatronics*, vol. 22, no. 3, pp. 1163–1173, 2017.

[9] ——, "Trajectory tracking control of an autonomous underwater vehicle using lyapunov-based model predictive control," *IEEE Transactions on Industrial Electronics*, vol. 65, no. 7, pp. 5796–5805, 2018.

[10] A. B. Martinsen, A. M. Lekkas, and S. Gros, "Reinforcement learning-based nmpc for tracking control of asvs: Theory and experiments," *Control Engineering Practice*, vol. 120, p. 105024, 2022.

[11] T. Fossen, *Handbook of Marine Craft Hydrodynamics and Motion Control*. Wiley, 2021.

[12] C. Marchaj, *Sail Performance: Techniques to Maximize Sail Power*. International Marine/McGraw-Hill, 2003.

[13] C. Liu, S. Yang, T. Duan, J. Huang, and Z. Wang, "Motion control of an one-meter class autonomous sailboat," in *2018 IEEE 8th International Conference on Underwater System Technology: Theory and Applications (USYS)*, 2018, pp. 1–6.

[14] Z. Feng, J. Qiu, H. Liu, Q. Sun, N. Ding, Z. Sun, T. L. Lam, and H. Qian, "An adaptive position keeping algorithm for autonomous sailboats," in *2019 IEEE International Conference on Robotics and Biomimetics (ROBIO)*, 2019, pp. 527–532.

[15] S. Han, J. Zhao, X. Li, J. Yu, S. Wang, and Z. Liu, "Online path planning for auv in dynamic ocean scenarios: A lightweight neural dynamics network approach," *IEEE Transactions on Intelligent Vehicles*, pp. 1–14, 2024.